

# Layered Hydrogen Titanate Nanowires with Novel Lithium Intercalation Properties

Junrong Li,<sup>†,‡</sup> Zilong Tang,<sup>†</sup> and Zhongtai Zhang<sup>\*,†</sup>

State Key Laboratory of New Ceramics and Fine Processing, Department of Materials Science and Engineering, Tsinghua University, Beijing 100084, People's Republic of China, and Beijing Institute of Space Medico-Engineering, Beijing 100094, People's Republic of China

Received July 23, 2005. Revised Manuscript Received August 31, 2005

Layered hydrogen titanate nanowires were synthesized from  $\text{TiO}_2$  via an alkaline–hydrothermal process and subsequent acid treatment. The average diameter of as-prepared nanowires is about 100 nm with a uniform interlayer spacing of 0.81 nm. The framework of this hydrogen titanate nanowires holds the composition of  $\text{H}_2\text{Ti}_3\text{O}_7$  as determined by thermogravimetric analysis. The nanostructured electrode made from these nanowires shows large lithium intercalation capacity (reversible lithium intercalation with  $\text{Li}_{0.71}\text{H}_{2/3}\text{TiO}_{7/3}$ ), high discharge/charge rate capability, and excellent cycling stability, as revealed by galvanostatically charge/discharge cycling tests. The detailed cyclic voltammetric investigation, however, indicates that the hydrogen titanate nanowires show pseudocapacitive characteristic during the  $\text{Li}^+$  insertion process. The novel electrochemical properties of hydrogen titanate nanowires are attributed to the open layered structure with a much larger interlayer spacing than normal intercalation compounds for commercial lithium ion batteries. The layered hydrogen titanate nanowires with unique electrochemical performance may become a promising lithium intercalation material for high-energy rechargeable lithium ion batteries and electrochemical supercapacitors.

## Introduction

There has been increasing interest in developing nanoscale electrode material for application in electrochemical devices and, in particular, rechargeable lithium batteries, due to much promise held by the nanostructured systems for future development in lithium ion battery technology, yielding high energy density, high discharge/charge rate capabilities, long cycle life, and excellent low temperature performance.<sup>1–3</sup> It is generally accepted that these limitations in the rate capabilities of Li ion batteries are mainly ascribed to slow solid-state diffusion of  $\text{Li}^+$  within the electrode materials.<sup>4</sup> Electrodes made from one-dimensional nanostructured (nanotube, wire, rod or belt) materials or mesoporous nanocomposites usually hold unique rate capabilities for lithium ion batteries, because the distance that  $\text{Li}^+$  must diffuse is restricted to the small radius direction, which is significantly smaller than that in usual powder made electrode.<sup>5,6</sup> As a result, there is tremendous current research interest in the development of nanostructured Li ion battery electrode materials with high capacity and excellent cycling stability.<sup>7–9</sup> There are a number of nanoscale transition metal oxides with

layered structure to be tested as lithium ion intercalation hosts.<sup>10,11</sup> Nanostructured or orderly organized mesoporous  $\text{TiO}_2$  electrodes have showed unique performance as lithium intercalation materials.<sup>12–14</sup> The behaviors of electrochemical lithium intercalation into  $\text{TiO}_2$  electrodes have been well addressed.<sup>15,16</sup>

Recently, titanate nanotubes<sup>17,18</sup> and nanowires<sup>19,20</sup> have attracted much attention, because of the wide applications of titanium oxide and relative simple preparation procedures to scale-up to fulfill the requirements of various applications. Hydrogen titanate nanotubes can be prepared from poly-

\* Corresponding author. Tel.: +8610-6277 2623; fax: +8610-6278 3046. E-mail: ljz02@mails.tsinghua.edu.cn.

<sup>†</sup> Tsinghua University.

<sup>‡</sup> Beijing Institute of Space Medico-Engineering.

- (1) Tarascon, J. M.; Armand, M. *Nature (London)* **2001**, *414*, 359.
- (2) Poizot, P.; Laruelle, S.; Grugeon, S.; Dupont, L.; Tarascon, J. M. *Nature (London)* **2000**, *407*, 496.
- (3) Sides, C. R.; Martin, C. R. *Adv. Mater.* **2005**, *17*, 125.
- (4) Bruce, P. G. *Chem. Commun.* **1997**, *19*, 1817.
- (5) Sides, C. R.; Li, N.; Patrissi, C. J.; Scrosati, B.; Martin, C. R. *MRS Bull.* **2002**, *26*, 604.
- (6) Zhou, H.; Li, D.; Hibino, M.; Honma, I. *Angew. Chem., Int. Ed.* **2005**, *44*, 797.

- (7) Li, N.; Mitchell, C. D.; Lee, T. K. P.; Martin, C. R. *J. Electrochem. Soc.* **2003**, *150*, A979.
- (8) Doble, A.; Ngala, K.; Yang, S. F.; Zavalij, P. Y.; Whittingham, M. S. *Chem. Mater.* **2001**, *13*, 4382.
- (9) Singhal, A.; Skandan, G.; Amatucci, G.; Badway, F.; Ye, N.; Manthiram, A.; Ye, H.; Xu, J. J. *J. Power Sources* **2004**, *129*, 38.
- (10) Zak, A.; Feldman, Y.; Lyakhovitskaya, V.; Leitius, G.; Popovitz-Biro, R.; Wachtel, E.; Cohen, H.; Reich, S.; Tenne, R. *J. Am. Chem. Soc.* **2002**, *124*, 4747.
- (11) Nordlinder, S.; Edstrom, K.; Gustafsson, T. *Electrochem. Solid-State Lett.* **2001**, *4*, A129.
- (12) Kavan, L.; Fattakhova, D.; Krtil, P. *J. Electrochem. Soc.* **1999**, *146*, 1375.
- (13) Kavan, L.; Rathousky, J.; Grätzel, M.; Shklover, V.; Zukal, A. *J. Phys. Chem. B* **2000**, *104*, 12012.
- (14) Sudant, G.; Baudrin, E.; Larcher, D.; Tarascon, J.-M. *J. Mater. Chem.* **2005**, *15*, 1263.
- (15) Wagemaker, M.; Kentgens, A. P. M.; Mulder, F. M. *Nature (London)* **2002**, *418*, 397.
- (16) Lindström, H.; Södergren, S.; Solbrand, A.; Rensmo, H.; Hjelm, J.; Hagfeldt, A.; Lindquist, S. E. *J. Phys. Chem. B* **1997**, *101*, 7717.
- (17) Kasuga, T.; Hiramatsu, M.; Hoson, A. *Langmuir* **1998**, *14*, 3160.
- (18) Du, G. H.; Chen, Q.; Che, R. C.; Yuan, Z. Y.; Peng, L. M., *Appl. Phys. Lett.* **2001**, *79*, 3702.
- (19) Zhang, Y. X.; Li, G. H.; Jin, Y. X.; Zhang, Y.; Zhang, J.; Zhang, L. D. *Chem. Phys. Lett.* **2002**, *365*, 300.
- (20) Du, G. H.; Chen, Q.; Han, P. D.; Yu, Y.; Peng, L. M. *Phys. Rev. B* **2003**, *67*, 035323.

morph of  $\text{TiO}_2$  by a simple alkaline–hydrothermal treatment and subsequent acid washing.<sup>21</sup> It was believed that the products were composed of anatase  $\text{TiO}_2$  at one time.<sup>22</sup> Later work suggested that the nanotubes were composed of the layered titanate  $\text{H}_2\text{Ti}_3\text{O}_7$ ,<sup>23–25</sup> or a family of layered hydrogen titanate with a general formula of  $\text{H}_2\text{Ti}_n\text{O}_{2n+1}\cdot\text{H}_2\text{O}$ .<sup>26</sup> An alternative of this material is orthorhombic  $\text{H}_x\text{Ti}_{2-x/4}\square_{x/4}\text{O}_4\cdot\text{H}_2\text{O}$  ( $x \approx 0.7$ ,  $\square$  = vacancy) with the lepidocrocite-type structure.<sup>27</sup> Bruce and co-workers reported the formation of titanate nanowires and the conversion to  $\text{TiO}_2$ -B nanowires by subsequent annealing.<sup>26</sup> This  $\text{TiO}_2$ -B electrode showed a very high specific charge storage capacity of 275 mAh/g and high rate capabilities for lithium intercalation by galvanostatic methods, which was much higher than that in normal  $\text{TiO}_2$ -B electrode and nanostructured anatase.<sup>28</sup> Kavan's group has recently tested the lithium storage in nanostructured anatase-type  $\text{TiO}_2$  prepared from  $\text{TiCl}_4$  via alkaline–hydrothermal treatment at 250 °C.<sup>29</sup> They predicted that the as-prepared nanostructured anatase  $\text{TiO}_2$  could store large capacity, up to ca. 800 C/g (about 222 mAh/g) from the detailed cyclic voltammetric investigation. They also tested the lithium insertion properties of phase-pure  $\text{TiO}_2$ -B with microfibrillar morphology prepared from amorphous  $\text{TiO}_2$ ; the results indicate that Li insertion into  $\text{TiO}_2$ -B is governed by a pseudocapacitive faradic process, the rate of which is not limited by solid-state diffusion of  $\text{Li}^+$  in a broad interval of scan rates.<sup>30</sup>

In the present study, we focus on the preparation and structural characterization of hydrogen titanate nanowires with layered structure and the electrochemical investigation of the lithium intercalation properties of nanostructured electrode made from these nanowires. Especially, detailed cyclic voltammetric measurements were performed to determine the kinetic behaviors of lithium storage in hydrogen titanate nanowires. Our previous work showed that a nanostructured electrode made from hydrogen titanate nanotubes holds unique lithium intercalation properties, with high capacity, high rate capabilities, and excellent cycling stability.<sup>31</sup> Both hydrogen titanate nanotubes and nanowires are derived from similar procedures; however, they may hold different local lattice structure, as evidenced by their transformation into different products after heat treatment (nanotubes to anatase, and nanowires to  $\text{TiO}_2$ -B<sup>26</sup>). Hydrogen titanate contains zigzag ribbons of  $\text{TiO}_6$  octahedra that share

edges with others;<sup>32</sup> the layer-by-layer stacking of titanate nanosheets may result in titanate nanowires with an open layered framework and tunnelike structure. Furthermore, the hydrogen titanate nanowires seem more stable than their nanotubes counterpart, because the framework of nanotubes is prone to be destroyed by acid or heat treatment,<sup>24</sup> while the nanowire is stable for heat treatment.<sup>26</sup> This hydrogen titanate is different from the typical oxides for lithium ion battery electrode materials in composition and structure to some extent.<sup>33</sup> The open layered structure and good chemical/thermal stability of hydrogen titanate nanowires triggered our investigation of the characteristic of lithium intercalation in these titanate nanowires in detail.

## Experimental Section

**Preparation of Materials.** Hydrogen titanate nanowires were synthesized by a sonochemical–hydrothermal reaction in concentrated NaOH aqueous solution, with a slight difference from the preparation of hydrogen titanate nanotubes shown in ref 23. The higher concentration of NaOH solution (15 M) and/or higher hydrothermal temperature (150–180 °C) and longer hydrothermal time (at least 72 h) than those for preparation of titanate nanotubes may result in nanowires. The white product was acid-washed, which involved washing the sample with dilute  $\text{HNO}_3$  solution and aging at pH = 5–6 for at least 8 h at room temperature. The material was then filtered and washed with distilled water and ethanol, respectively. Then the white fluffy product was dried in a vacuum at 80 °C for at least 3 h, to remove the labile absorbed  $\text{H}_2\text{O}$  completely.

**Preparation of Electrodes.** Electrochemical properties were measured on electrodes prepared using mixtures comprising 80 wt % active material, 10 wt % acetylene black, and 10 wt % polyvinylidene fluoride (PVDF) binder. The electrode films were fabricated by the doctor-blade technique on aluminum foil. After predrying at 80 °C, the electrode film was hot pressed at 120–150 °C and then completely dried in a vacuum oven at 120 °C for at least 4 h to remove the trace absorbed water in the electrode lamella. The electrode lamellas were cut into disks of 0.83 cm<sup>2</sup>. The loading amount of the active material was 2–3 mg/cm<sup>2</sup>.

**Characterization of Samples.** Transmission electron microscopy (TEM) was performed on a JEOL JEM-200CX. High-resolution transmission electron microscopy (HRTEM) was performed on a TECNAI F30 (Philips). Powder X-ray diffraction (XRD) was performed on a Rigaku D/max-RB diffractometer operating in transmission mode with Cu K $\alpha$  radiation ( $\lambda = 1.5418 \text{ \AA}$ ). Raman spectra was excited by an Ar<sup>+</sup> laser at 514 nm and recorded on a RM2000 spectrometer (Renishaw). Microscopic measurements allowed the different sampled areas (different grains of the solid material) to be focused on to test the homogeneity of studied samples. Scanning electron microscopy was performed on a JEOL JSM-6301F equipped with a field emission gun (FEG-SEM). The BET specific surface area was measured by the  $\text{N}_2$  adsorption/desorption method at liquid nitrogen temperature performed on a Quantachrome NOVA 4000. Quantitative elemental analysis was performed on a Shimadzu XRF-1800. Thermogravimetric analysis (TG) was performed on a SETARAM-TGA92 in the temperature range from room temperature to 860 °C. The real density of the hydrogen titanate nanowires was measured on a Micromeritics AccuPyc 1330; the measured real density is an average value

- (21) Kasuga, T.; Hiramatsu, M.; Hoson, A.; Sekino, T.; Niihara, K. *Adv. Mater.* **1999**, *15*, 1307.
- (22) Yao, B. D.; Chan, Y. F.; Zhang, X. Y.; Zhang, W. F.; Yang, Z. Y.; Wang, N. *Appl. Phys. Lett.* **2003**, *82*, 281.
- (23) Chen, Q.; Zhou, W. Z.; Du, G. H.; Peng, L. M. *Adv. Mater.* **2002**, *14*, 1208.
- (24) Sun, X.; Li, Y. *Chem. Eur. J.* **2003**, *9*, 2229.
- (25) Zhang, S.; Peng, L. M.; Chen, Q.; Du, G. H.; Dawson, G.; Zhou, W. Z. *Phys. Rev. Lett.* **2003**, *91*, 256103.
- (26) Armstrong, A. R.; Armstrong, G.; Canales, J.; Bruce, P. G. *Angew. Chem., Int. Ed.* **2004**, *43*, 2286.
- (27) Ma, R.; Bando, Y.; Sasaki, T. *Chem. Phys. Lett.* **2003**, *380*, 577.
- (28) Armstrong, A. R.; Armstrong, G.; Canales, J.; Garcia, R.; Bruce, P. G. *Adv. Mater.* **2005**, *17*, 862.
- (29) Kavan, L.; Kalbac, M.; Zukalova, M.; Exnar, I.; Lorenzen, V.; Nesper, R.; Grätzel, M. *Chem. Mater.* **2004**, *16*, 477.
- (30) Zukalova, M.; Kalbac, M.; Kavan, L.; Exnar, I.; Nesper, R.; Grätzel, M. *Chem. Mater.* **2005**, *17*, 1248.
- (31) Li, J.; Tang, Z.; Zhang, Z. *Electrochem. Commun.* **2005**, *7*, 62.

- (32) Zhu, H.; Gao, X.; Lan, Y.; Song, D.; Xi, Y.; Zhao, J. *J. Am. Chem. Soc.* **2004**, *126*, 8380.
- (33) Whittingham, M. S. *Chem. Rev.* **2004**, *104*, 4271.

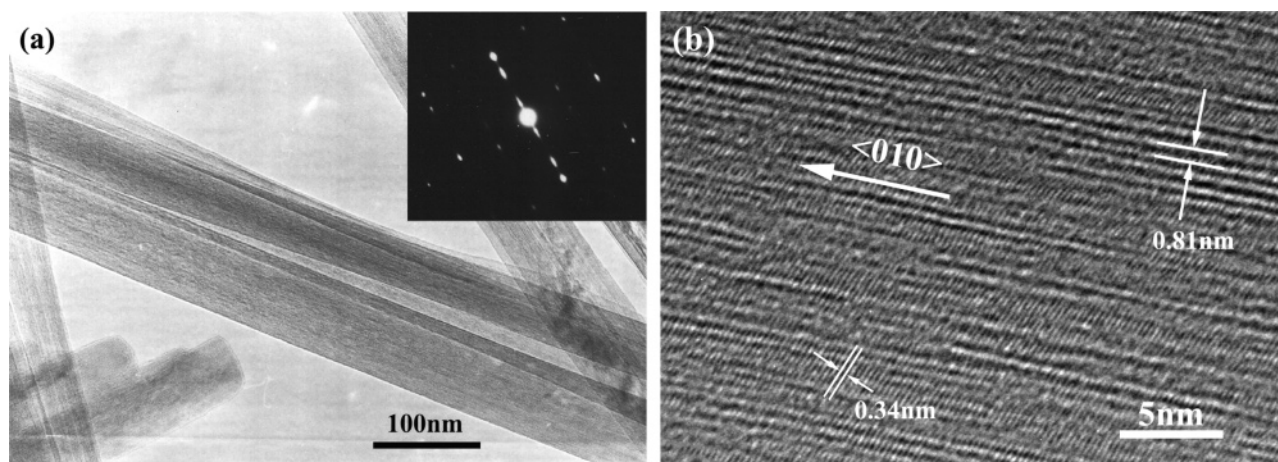


**Figure 1.** (a) Low-resolution TEM image of hydrogen titanate nanowires (top right inset is a selected-area electron diffraction pattern of a single nanowire); (b) HRTEM micrograph of as-prepared hydrogen titanate nanowires, clearly showing the layered structure with an interlayer spacing of 0.81 nm.

determined by testing samples five times to reduce the measuring errors.

**Measurement of Electrochemical Performances.** The cells consisted of the electrode, a lithium metal counter electrode, and the electrolyte of a 1 M solution of  $\text{LiPF}_6$  in ethylene carbonate/dimethyl carbonate (1:1 v/v; Merck). The cells were constructed and handled in an Ar-filled glovebox and were evaluated using coin-type cells (CR2032). Electrochemical measurements were carried out using a LAND Celltest-2001A (Wuhan, China) system. The cells were galvanostatically discharged and charged between 2.5 and 1 V vs the Li counter electrode. A cyclic voltammogram was recorded from 3.0 to 1.0 V using an IM6 electrochemical workstation, with a 1 M solution of  $\text{LiPF}_6$  in ethylene carbonate/dimethyl carbonate (1:1 v/v; Merck) as electrolyte and counter and reference electrodes of Li metal disk.

## Results and Discussion

**Characterization of Materials.** The alkaline–hydrothermal approach provides a simple, massive production method to convert  $\text{TiO}_2$  polymorph into slim titanate nanotubes. The prepared titanate nanotubes hold layered wall structure with the interlayer spacing of about 0.78 nm.<sup>23</sup> Here we have successfully prepared titanate nanowires with layered structure using similar alkaline–hydrothermal processing and subsequent acid washing. Figure 1 shows typical TEM (a) and HRTEM (b) images of the as-prepared hydrogen titanate nanowires. The TEM image clearly shows that the diameter of the hydrogen titanate nanowires is about 100 nm, and its length can reach several micrometers. The diameter of the nanowires is much smaller than the dimensional size of commercial lithium ion battery cathode materials, which is usually in the range of several to tens of micrometers. The HRTEM microgram shows clearly the well-crystallized layered structure of hydrogen titanate nanowires with the interlayer spacing of about 0.81 nm, which is slightly larger than that of titanate nanotubes;<sup>23</sup> however, this layered titanate lattice was usually prepared from a high-temperature solid-state reaction.<sup>34</sup> The difference in interlayer spacing between nanotubes and nanowires may be mainly attributed to the structural difference between the former, with a

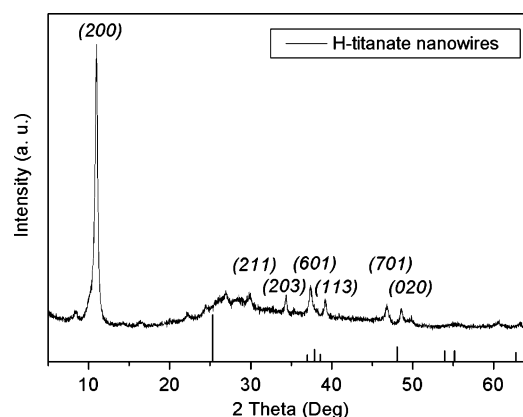


**Figure 2.** Typical XRD profile of as-prepared hydrogen titanate nanowires. The black bars from the bottom indicate diffraction peaks of the starting anatase  $\text{TiO}_2$ .

scrolling cross section, and the latter, with a layer-by-layer stacking framework. The axis of the nanowire is in the  $\langle 010 \rangle$  direction, and the layer stacking is parallel to this direction. The real density of as-prepared hydrogen titanate is 3.05  $\text{g}/\text{cm}^3$ , as measured by a Micromeritics AccuPyc 1330, which is much less than that of anatase or rutile, indicating the open and loose structure of as-prepared hydrogen titanate nanowires. The SAED pattern of a single nanowire also indicates the layered structure of as-prepared hydrogen titanate nanowires, which is in agreement with the results of Bruce.<sup>26</sup> There is no residual sodium ion detected in the hydrogen titanate nanowires by XRF quantitative characterization, which implies it is effective to convert sodium titanate nanowires into hydrogen titanate nanowires topochemically by acid washing and aging processing.

Figure 2 shows a typical XRD profile of as-prepared nanowires and standard X-ray diffraction peaks of starting anatase  $\text{TiO}_2$ . The result shows that the as-prepared nanowires are not  $\text{TiO}_2$  yet but have features similar to those of hydrogen titanate with monoclinic lattice ( $C2/m$ ) reported in ref 32. The detailed TG analysis results (shown in Figure 3) indicate that the as-prepared titanate nanowires hold a composition of  $\text{H}_2\text{Ti}_3\text{O}_7$ . The peak of (200) is much higher than other peaks in the reflections, implying the regular layered structure and high orientation of this nanostructure. The calculated  $d_{200}$  value of 8.07 Å from this XRD profile

(34) Sasaki, T.; Watanabe, M.; Hashizume, H.; Yamada, H.; Nakazawa, H. *J. Am. Chem. Soc.* **1996**, *118*, 8329.



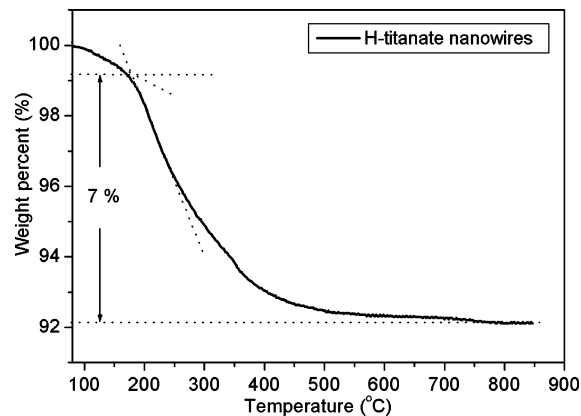


**Figure 3.** TG plot of hydrogen titanate nanowires in an air stream immediately after the sample is fresh dried for at least 4 h.

is well in agreement with the interlayer spacing from HRTEM characterization results.

TG analysis was performed in a TG-DTA system in air stream immediately after the sample was fresh dried in a vacuum oven at 80 °C for at least 4 h. The weight loss before 200 °C is mainly attributed to the desorption of surface adsorbed water. About 7% weight loss of the as-prepared nanowires after 200 °C is mainly due to the hydrogen titanate decomposing into  $\text{TiO}_2$  and  $\text{H}_2\text{O}$ ; thus, we can assume that the prepared hydrogen titanate nanowires hold the composition with  $\text{H}_2\text{Ti}_3\text{O}_7$  (with a standard 6.9% weight loss). On the other hand, this result also indicates that the  $\text{H}_2\text{O}$  in the titanate nanowire framework is stable enough for vacuum-drying at 80–120 °C. Bruce and co-workers showed that titanate nanowires could be converted to  $\text{TiO}_2$ -B phase by subsequent heat treatment but still retain the nanowire shape.<sup>26</sup> This may imply that the thermal stability of titanate nanowires is superior to that of their nanotube counterparts, which may make these hydrogen titanate nanowires more practical in applications than titanate nanotubes. Because the hydrogen titanate nanotubes prepared by a similar alkaline-hydrothermal approach can be changed into  $\text{TiO}_2$  with anatase structure,<sup>35</sup> other than  $\text{TiO}_2$ -B, this may indicate that the lattice structure of hydrogen titanate nanowires is different from that of nanotubes, although both of them hold a layered structure. This may also account for the difference in thermal stability between hydrogen titanate nanowires and nanotubes.

Further insight into the phase composition of the hydrogen titanate nanowires can be obtained from microscopic confocal Raman spectroscopy. This technique allows selecting a sampled area of several micrometers in size, and by scanning of the sample surface, we can distinguish the homogeneity of composition in the sample. Figure 4 displays illustrative examples of as-prepared hydrogen titanate nanowires. The Raman spectra acquired at different spots keep the same profile, that of pure hydrogen titanate. No anatase or rutile  $\text{TiO}_2$  can be detected in different areas of this sample, which indicates that the starting  $\text{TiO}_2$  has been fully converted into hydrogen titanate nanowires by the low-temperature alkaline-hydrothermal approaches. In fact, the reaction conditions for preparing nanowires are more rigorous than for their nanotube counterparts both in hydrothermal temperature and

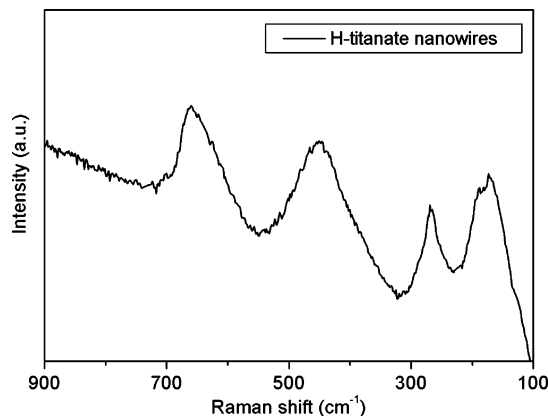


**Figure 4.** Micro-Raman spectra of as-prepared hydrogen titanate nanowires.

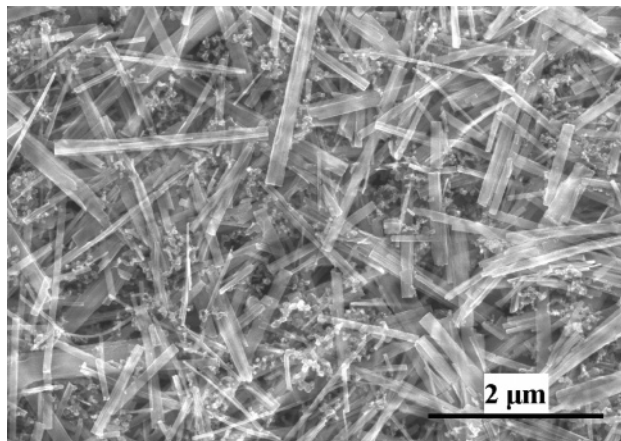


**Figure 5.** FEG-SEM micrograph of electrode film prepared by the doctor-blading technique from hydrogen titanate nanowires and conductive acetylene black.

concentration of NaOH, which may make sure that the  $\text{TiO}_2$  precursor is completely transformed into titanate. This phase-pure sample will benefit the subsequent electrochemical investigation of nanostructured electrodes made from these nanowires.

Because of the high surface energy and large specific surface area of nanostructured materials ( $S_{\text{BET}} = 152.6 \text{ m}^2/\text{g}$  for hydrogen titanate nanowires), they have strong tendency to adsorb water when exposed in air atmosphere, so they must be dried in a vacuum oven completely before fabricating the electrode film to remove surface adsorbed water. To avoid agglomeration with each other during fabrication of the electrode, a facile in situ ultrasonic dispersion approach is adopted.<sup>31</sup> Figure 5 shows the FEG-SEM of the microstructure of the as-prepared well-dispersed electrode films after hot-press. It is obvious that the hydrogen titanate nanowires are well-dispersed, and conductive acetylene black dispersed homogeneously in the interspace between hydrogen titanate nanowires. This novel homogeneous structure of the electrode film may ensure good conductivity as well as compact contact between electrode and liquid electrolyte, thus facilitating lithium ion diffusion in the electrode, which will make the nanostructured electrode hold improved interfacial charge and lithium ion transfer characteristics.

**Electrochemical Properties by Galvanostatic Lithium Intercalation.** The galvanostatic cycling performance of electrode made from hydrogen titanate nanowires at different

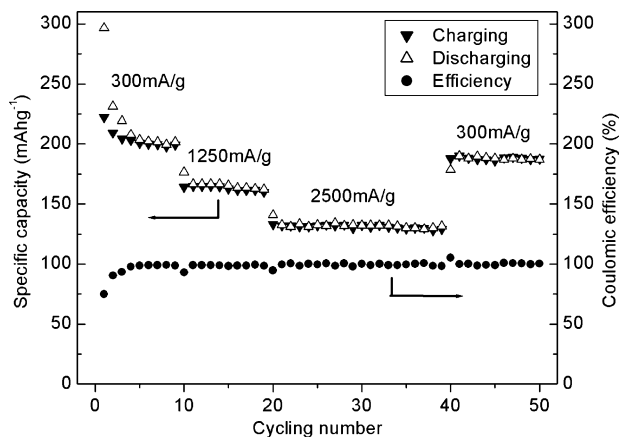


**Figure 6.** Galvanostatic cycling performance of hydrogen titanate nanowires electrode at different charging/discharging rates.

charge–discharge rates is displayed in Figure 6. The results show the high discharge rate capability and excellent cycling stability of this nanostructured electrode, although an obvious drop of discharge capacity can be observed during the first several discharge–charge cycles. The first discharge capacity can reach 296.6 mAh/g, which is larger than that in normal crystalline  $\text{TiO}_2$  electrodes.<sup>36,37</sup> When changing the charge/discharge current density, the capacity still can keep stable to a corresponding level. Here the electrode has shown a relative high average cycling discharge capacity of 191.8 mAh/g at 300 mA/g current density and can keep a very high capacity, even at high discharge rates (166.1 and 132.2 mAh/g at current density of 1250 and 2500 mA/g, respectively). Those charge/discharge current densities are already much larger than those in commercial lithium ion batteries nowadays. The large capacity, high rate capability, and excellent cycling stability of this nanostructured electrode made from hydrogen titanate nanowires indicate a novel kinetic performance different from those of anatase and commercial lithium ion batteries electrode materials. The behaviors of lithium intercalation in hydrogen titanate nanowires are similar to that of  $\text{TiO}_2$ -B nanowires with similar open structure.<sup>28</sup>

Figure 7 shows the first three cycles of the discharge/charge voltage profile vs capacity of electrode made from hydrogen titanate nanowires. The smoothly sloping nature of the voltage profiles indicates that lithium intercalation into the hydrogen titanate nanowires remains a single-phase process after repeated cycling, which means that no two phases are interfacial during the lithium intercalation process. This electrochemical performance is similar to that of potassium titanate nanowires prepared by alkaline–hydrothermal processes from Ti powders with good reversible lithium intercalation performance.<sup>38</sup> This similar electrochemical performance between hydrogen and potassium titanate nanowires may be ascribed to the common open layered and tunnelike structure. Because hydrogen titanate is lighter than potassium titanate in molar weight, the former

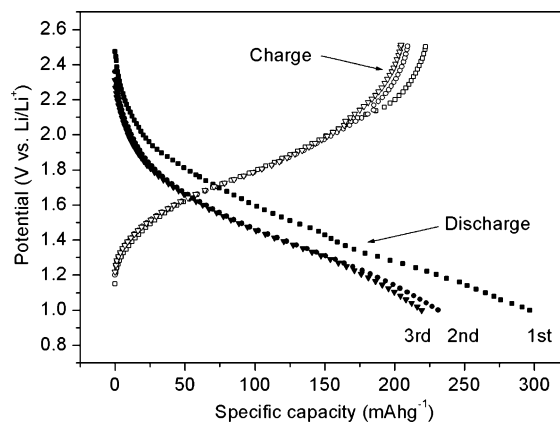


**Figure 7.** The first three cycles of galvanostatic discharge/charge voltage patterns of titanate nanowires electrode at a discharge/charge current density of 300 mA/g.

may hold larger theoretical specific capacity than the latter. The difference in reversible capacity between both nanowires (ca. 200 mAh/g for hydrogen titanate nanowires vs ca. 160 mAh/g for potassium titanate nanowires) may support this assumption. Furthermore, the potassium titanate nanowires are stable for reversible lithium intercalation and deintercalation in composition, morphology, and crystal structure.<sup>38</sup> The sloping feature of the charge/discharge profile is also similar to that of amorphous  $\text{MnO}_2$  with nanoporous texture, which will keep the amorphous state upon reversible lithium intercalation and deintercalation.<sup>39</sup> These amorphous structures with short-range order far from equilibrium may offer the advantages of kinetic stabilization in furnishing single-phase intercalation hosts that would exhibit very high reversible capacities and potentially superior cycling performance. This characteristic also observed in hydrogen titanate nanowires may make them hold both excellent cycling stability and high rate capability. On the contrary, both results may also imply the stability in composition, morphology, and structure of hydrogen titanate nanowires after reversible lithium intercalation and deintercalation.

#### Kinetics Investigation by Cyclic Voltammetric Method.

Figure 8 shows cyclic voltammograms (CV) of electrode made from hydrogen titanate nanowires between 1 and 3V. The appearance of kinetic effects depends on the scan rates. At small scan rates, systems may yield reversible waves, while at large scan rates, irreversible behavior is observed.<sup>40</sup> Here the cyclic voltammetric test was performed at the very small scan rate of 0.05 mV/s to ensure yielding quasi-reversible waves. Only broad redox peaks can be observed during the entire voltage range, even though the scan rate is very low, which is well in agreement with the sloping voltage profile during the discharge/charge cycles. There are notable differences between the first two cycles both in peak position and in integral voltammetric charge. The following cyclic voltammograms, however, keep almost the same shape as the second one, which may make us assume that the electrochemical lithium intercalation into and release from hydrogen titanate nanowires is kinetically reversible when

(36) Exnar, I.; Kavan, L.; Huang, S. Y.; Grätzel, M. *J. Power Sources* **1997**, *68*, 720.

(37) Wilhelm, O.; Pratsinis, S. E.; de Chambrier, E.; Crouzet, M.; Exnar, I. *J. Power Sources* **2004**, *134*, 197.

(38) Wang, B. L.; Chen, Q.; Hu, J.; Li, H.; Hu, Y. F.; Peng, L. M. *Chem. Phys. Lett.* **2005**, *406*, 95.

(39) Xu, J. J.; Ye, H.; Jain, G.; Yang, J. *Electrochem. Commun.* **2004**, *6*, 892.

(40) Bard, A. J.; Faulkner, L. R. *Electrochemical Methods: Fundamentals and Applications*; John Wiley & Sons: New York, 1980.

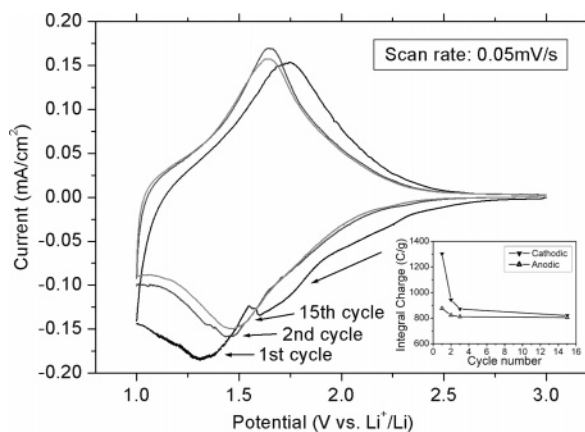


**Figure 8.** Cyclic voltammograms of hydrogen titanate nanowires electrode in 1 M LiPF<sub>6</sub> + EC/DMC (1/1, v/v) at a scan rate of 0.05 mV/s. (Bottom right inset: integral voltammetric charges from cyclic voltammograms are plotted against cycle number. The charge is normalized to the actual active materials loaded on the testing electrode.) The electrode geometric surface area is 0.83 cm<sup>2</sup>.

the sweeping rate is as low as 0.05 mV/s. The position of broad redox peaks is right, located in the S-peak ranges,<sup>29</sup> and the S-peaks have been denoted as characteristic of a capacitive charging process. This result may indicate that the lithium storage in layered hydrogen titanate nanowires may hold different kinetic features from normal anatase electrodes.<sup>13</sup>

The integral voltammetric charge change is another characteristic. The inset (bottom right) in Figure 8 displays the integral voltammetric charge normalized to the active materials loaded on the electrode. Investigation of the various cycles of the cathodic branch and anodic branch of CV curves shows that there is a dramatic drop of cathodic integral voltammetric charge during the first three cycles with a similar tendency as the galvanostatic charge/discharge capacity; however the capacity fade of the anodic integral voltammetric charge is much weaker than that of the cathodic one. The slow CV scan rates may reveal capacity at the quasiequilibrium state; therefore, the integral voltammetric charge may represent the reversible capacity well. Investigation of the CV profiles of hydrogen titanate nanowires and TiO<sub>2</sub> (anatase) nanotubes derived from the hydrogen titanate nanotubes annealed in 350 °C for 2 h showed both similar profile and similar capacity fade between the first two cathodic waves in the voltage ranges from 1.5 to 1.0 V.<sup>35</sup> Apparently, there is no proton in the framework of the TiO<sub>2</sub> nanotubes. So this dramatic capacity fade during the first two cathodic waves may mainly be ascribed to the nanostructured characteristic and have been attributed to the trace water adsorbed on the electrode surface because of the large specific surface area of hydrogen titanate nanowires and layered structure.<sup>35</sup> There is no obvious drop of integral voltammogram charge during the following cycles (15th cycle vs 3rd cycle), which is in accordance with the excellent cycling stability of this nanostructured electrode by galvanostatic discharge/charge methods. The stable reversible capacity is larger than 800 C/g when the Coulombic efficiency (ratio of extraction capacity to insertion capacity) reaches close to 100% from the cyclic voltammetric measurement, which is equivalent to that of nanostructured TiO<sub>2</sub><sup>29</sup> and much larger than that in a normal TiO<sub>2</sub> electrode.<sup>36</sup>

From the data obtained from CV measurements and galvanostatic discharge/charge tests, we can assume that the lithium ion intercalation into hydrogen titanate nanowires has the similar behavior as that of TiO<sub>2</sub>, as expressed by the following equations:



The reversible capacity of 800 C/g may indicate that the lithium insertion extent  $x$  is about 0.71, which is much larger than that in a normal anatase electrode, where  $x$  is usually limited to 0.5 at room temperature.

Cyclic voltammogram at various scan rates were also performed to further investigate the kinetic behavior of lithium storage in hydrogen titanate nanowires. To remove trace water and to avoid the influence of the side reaction, the electrode has been galvanostatically charged/discharged for several cycles before performing those cyclic voltammetric tests. Because of the relative high peak current when it was performed at high scan rates, the systematic deviation due to the uncompensated  $iR$  drop of the cell would increase greatly. To reduce this deviation, the CV was performed at relative small intervals (0.05–1.0 mV/s). Figure 9 displays cyclic voltammograms recorded with various scan rates (A) and the peak currents plotted against the scan rates (B). Apparently, the linear relationship between peak currents and scan rates indicates the characteristic for capacitive charging

$$i = dQ/dt = C dE/dt = C\nu \quad (2)$$

$Q$  is the voltammetric charge,  $C$  is capacitance, and  $dE/dt$  is the scan rate  $\nu$ . This CV profile, however, indicates a surface-confined charge-transfer process, which can be considered faradic pseudocapacitance. The pseudocapacitive behavior of S-peaks is readily explained in terms of the interaction taking place on the nanosheet surface.<sup>29</sup> Here the layered structure of hydrogen titanate nanowires also showed this interesting phenomenon. There are three plausible reasons to account for this novel kinetic performance. First, the high specific surface area of hydrogen titanate nanowires (152.6 m<sup>2</sup>/g), as well as the novel electrode morphology, will make a perfect contact between the nanostructured electrode and the nonaqueous liquid electrolyte, which will greatly improve the interfacial characteristic between electrode and the electrolyte. Because of the special morphology of this nanostructured electrode made from hydrogen titanate nanowires, the electrode morphology must be taken into account when considering the actual electrode area. From the FEG–SEM micrograph of the electrode shown in Figure 5, the hydrogen titanate nanowires are well-dispersed, with no obvious agglomeration among them to be found, so the liquid electrode can fill the interspace between nanowires. In other words, every hydrogen titanate nanowire is surrounded by liquid electrolyte. Thus, we can assume that the actual electrode is equal to the sum surface area of the outer surface of all loaded hydrogen titanate nanowires. So we can estimate the actual electrode area from the real density and the dimensional size of hydrogen titanate nanowires as well as the loaded amount with eq 3:

$$S = 4m/\rho d \quad (3)$$



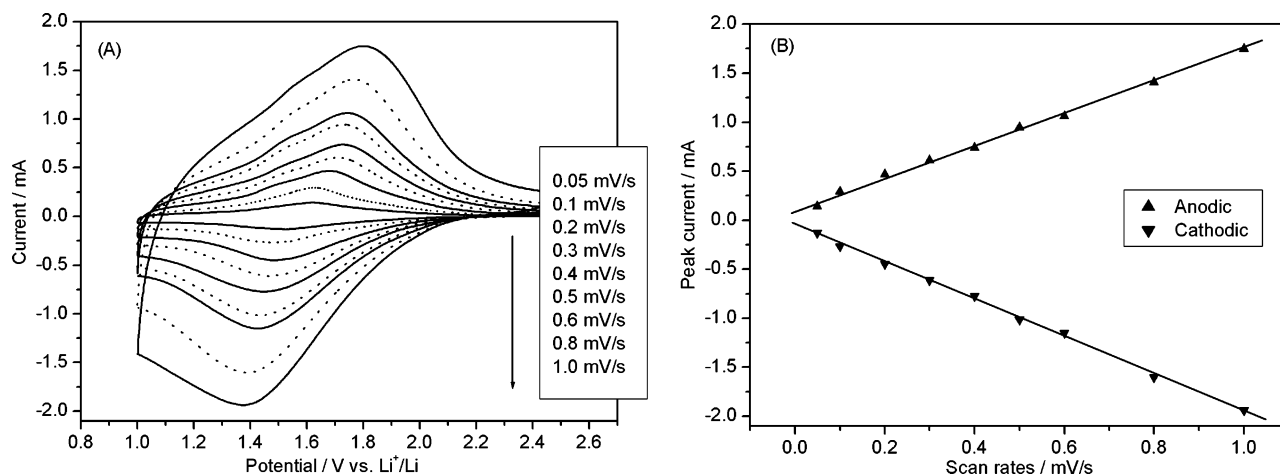


**Figure 9.** (A) Cyclic voltammograms of nanostructured electrode made from hydrogen titanate nanowires in 1 M LiPF<sub>6</sub> + EC/DMC (1/1, v/v) at various scan rates. The scan rates are 0.05, 0.1, 0.2, 0.3, 0.4, 0.5, 0.6, 0.8, and 1.0 mV/s, respectively. (B) The linear relationship between the anodic (▲) and cathodic (▼) peak currents and the scan rates. The electrode geometric surface area is 0.83 cm<sup>2</sup>.

Where  $S$  is actual electrode area in cm<sup>2</sup>,  $m$  is loading active material mass in gram,  $\rho$  is real density of hydrogen titanate nanowires in g/cm<sup>3</sup>, and  $d$  is the average diameter of nanowires in cm. The real density of as-prepared hydrogen titanate nanowires is 3.05 g/cm<sup>3</sup>, as measured by a Micromeritics AccuPyc 1330; the average diameter of titanate nanowires is 100 nm (10<sup>-5</sup> cm). The surface area of the end face may be neglected because of the high aspect ratio of these nanowires. The loading of active material in the electrode with a geometric area of 0.83 cm<sup>2</sup> is 2.024 mg; we can calculate the actual electrode area of 265.4 cm<sup>2</sup> with eq 3. This indicates that the actual electrode area is estimated to be almost 300 times larger than the geometric area of the electrode.

Second, the slim diameter of the hydrogen titanate nanowires will greatly reduce the distance of lithium ion diffusion in the solid state compared to a normal lithium ion battery electrode derived from a high-temperature solid-state reaction. Both TEM and SEM characterization results show the as-prepared hydrogen titanate nanowires with an average diameter of about 100 nm, which is much smaller than the dimensional size of the current lithium ion battery electrode material, with a particle dimensional size up to several to tens of micrometers.

Finally, the interlayer spacing in hydrogen titanate nanowires is much larger than that in normal transitional metal oxide intercalation compounds, which will also facilitate the lithium ion diffusion in this open and loose structure. Hydrogen titanate nanotubes and nanowires are derived from the same TiO<sub>2</sub> and similar alkaline–hydrothermal approach, but with different morphology and structure, and they showed similar kinetics of electrochemical lithium intercalation. The common feature between them lies in both of them holding layered structure with similar interlayer spacing, with scrolling structure for nanotubes and layer-by-layer stacking structure for nanowires. But they may hold different local lattice structure, because hydrogen titanate nanotubes will be transformed into anatase by heating,<sup>35</sup> while nanowires become TiO<sub>2</sub>-B.<sup>26</sup> This open layered structure, however, will provide a very large accessible surface area for lithium storage but also a more open tunnel than normal intercalation

materials. This layered structure of hydrogen titanate nanowires will account for the unique electrochemical kinetics for lithium intercalation. The novel pseudocapacitive feature of this nanostructured electrode, as well as the high charge/discharge capacity and high rate capability, may give this electrode potential applications in high-performance rechargeable lithium ion batteries and high-power electrochemical supercapacitors.<sup>41–43</sup>

This pseudocapacitive characteristic, however, is very similar to that of newly reported TiO<sub>2</sub>-B.<sup>30</sup> In fact, the hydrogen titanate nanowires can be transformed into TiO<sub>2</sub>-B nanowires by subsequent heating treatment;<sup>26</sup> this may show the common feature in structure and hence the electrochemical properties. There are several TiO<sub>2</sub> materials with orderly organized mesoporous morphology and nanoporous or nanocrystalline structure that also showed this unique pseudocapacitive property, and now the layered hydrogen titanate nanowires also showed this unique characteristic. Accordingly, the question arises if there is any common feature among these TiO<sub>2</sub> materials and hydrogen titanate originating from different sources with similar lithium intercalation kinetics? If so, what is this common feature? So it is worth further investigating the correlation between the structure and the electrochemical properties of hydrogen titanate nanowires/nanotubes and TiO<sub>2</sub>-B.

## Conclusions

In summary, layered hydrogen titanate nanowires with uniform morphology were successfully synthesized from TiO<sub>2</sub> via an alkali–hydrothermal process. Different from the scrolling structure of hydrogen titanate nanotubes, nanowires have a layer-by-layer stacking structure. The average diameter of as-prepared nanowires is about 100 nm with a uniform interlayer spacing of 0.81 nm. The detailed TG analysis shows the framework of this hydrogen titanate nanowires with the composition of H<sub>2</sub>Ti<sub>3</sub>O<sub>7</sub>. Both galvanostatic cycling

(41) Du Pasquier, A.; Laforge, A.; Simon, P.; Amatucci, G.; Fauvarque, J. J. *Electrochem. Soc.* **2002**, *149*, A302.

(42) Prasad, K. R.; Miura, N. *Appl. Phys. Lett.* **2004**, *85*, 4199.

(43) Winter, M.; Brodd, R. J. *Chem. Rev.* **2004**, *104*, 4245.

tests and cyclic voltammetric measurement show that the as-prepared nanowires can accommodate lithium as high as  $\text{Li}_{0.71}\text{H}_{2/3}\text{TiO}_{7/3}$ , reversibly. The electrode can work smoothly at various charge/discharge current densities and even at very high discharge current density; hence, they have an excellent high rate cycling stability. The detailed cyclic voltammetric investigations, however, indicate that the lithium insertion into hydrogen titanate nanowires is governed by a pseudocapacitive Faradic process, which means that the rate-limiting factors do not lie in the solid-state diffusion of  $\text{Li}^+$  ion in a broad interval of scan rates. Three plausible factors, including the structure and dimensional size of the intercalation host and the morphology of the nanostructured electrode, are attributed to improved kinetics of this nanostructured elec-

trode. This hydrogen titanate nanowire with layered structure may become a promising candidate as a novel lithium storage material.

**Acknowledgment.** This work was supported by National High Tech Research & Development Program (Grant No. 2003AA302320) and National Natural Science Funds of China (Grant Nos. 50372033 and 50472005), as well as the Basic Research Funds of Tsinghua University (Grant No. JC2003040). We also thank Dr. Wang, R. M. of Electron Microscopy Laboratory at Peking University for his help with the HRTEM characterization.

CM0516199